The joint helicity-energy cascade for homogeneous, isotropic turbulence generated by approximate deconvolution models

William J. Layton[1,5] Carolina C. Manica[2,5]

Monika Neda[3,5] Leo G. Rebholz[4,5]

Department of Mathematics

University of Pittsburgh PA 15260

May 30, 2006

keywords: LES, deconvolution, joint cascade, energy, helicity, turbulence

AMS subject classifications: 76F05, 76F65, 76M55

Abstract

In the large, getting a prediction of a turbulent flow right means getting the energy balance correct and getting the rotational structures correct. In two-dimensional flows this means (in the large) matching the energy and enstrophy statistics. In this report we consider a family of large eddy simulation approximate deconvolution models of turbulence. Based on a rigorous analysis of their kinetic energy and helicity balance, see [17], [27], Dunca and Epshteyn [9], we apply similarity theory to the model. We show that the model has a helicity cascade, linked to its energy cascade developed in [20], satisfying

$$\text{Helicity}(k) \sim \epsilon_{model}^{2/3} k^{-5/3} \quad \text{and} \quad \text{Energy}(k) \sim \gamma_{model} \epsilon_{model}^{-1/3} k^{-5/3} \quad \text{over } 0 < k < 1/\delta$$

[1]wjl@pitt.edu, http://www.pitt.edu/~wjl

[2]cac15@pitt.edu, http://www.pitt.edu/~cac15

[3]mon5@pitt.edu, http://www.pitt.edu/~mon5

[4]ler6@math.pitt.edu, http://www.math.pitt.edu/~ler6

$$\text{Helicity}(k) \sim \epsilon_{model}^{2/3} \delta^{-2} k^{-11/3} \quad \text{and} \quad \text{Energy}(k) \sim \gamma_{model} \epsilon_{model}^{-1/3} \delta^{-2} k^{-11/3} \quad \text{over } k > 1/\delta$$

where δ is the filter width. Thus, the method predicts the correct helicity statistics up to the cutoff frequency. We also discuss the existence of a helicity microscale.

The analysis is carried out for differential filters. We conclude by describing how the results are modified for other, general filters.

1 Introduction

Direct numerical simulation of many turbulent flows is not feasible for the foreseeable future within time and resource constraints of many applications. There are thus many approaches to finding reduced models of turbulent flows whose solutions have a smaller number of persistent scales (and thus can be solved more quickly and economically). However, the associated closure problem cannot be solved exactly. Thus, it is possible (and in fact not uncommon) that a given turbulence model's solution has little physical fidelity, quantitative agreement and qualitative agreement with the flow averages sought.

We consider herein aspects of flow statistics and the physical fidelity related to the coherent rotational structures and integral invariants (helicity and helicity statistics) predicted by a family of parameter free large eddy simulation models of turbulence. Broadly, if δ is the (user-selected) filter length scale and *overbar* denotes the associated local, spacial averaging, the true averages, $\overline{\mathbf{u}}$, $\overline{p}$, of an incompressible viscous fluid satisfy the well known Space Filtered Navier-Stokes equations given by

$$\overline{\mathbf{u}}_t + \nabla \cdot (\overline{\mathbf{u}\,\mathbf{u}}) - \nu \Delta \overline{\mathbf{u}} + \nabla \overline{p} = \overline{\mathbf{f}} \qquad \text{and} \qquad \nabla \cdot \overline{\mathbf{u}} = 0. \tag{1}$$

The closure problem (which occurs since $\overline{\mathbf{u}\,\mathbf{u}} \neq \overline{\mathbf{u}}\,\overline{\mathbf{u}}$) thus leads to the deconvolution problem:

$$\text{given } \overline{\mathbf{u}}, \text{ find } \mathbf{u} \text{ (approximately).} \tag{2}$$

Calling this approximate deconvolution of $\mathbf{u}$, $D(\overline{\mathbf{u}})$:

$$\text{approximation to } \mathbf{u} = D(\overline{\mathbf{u}}),$$

an approximate solution to the closure problem is then $\overline{\mathbf{u}\,\mathbf{u}} \approx \overline{D(\overline{\mathbf{u}})\,D(\overline{\mathbf{u}})}$. The LES model induced is to find $(\mathbf{w}, q)$ (sought to approximate $(\overline{\mathbf{u}}, \overline{p})$) satisfying

$$\mathbf{w}_t + \nabla \cdot (\overline{D(\mathbf{w})\,D(\mathbf{w})}) - \nu \Delta \mathbf{w} + \nabla q = \overline{\mathbf{f}} \qquad \text{and} \qquad \nabla \cdot \mathbf{w} = 0 \tag{3}$$

with initial condition $\mathbf{w}(x, 0) = \mathbf{w}_0(x)$. Here we take $\Omega = (0, L)^3$ and impose periodic boundary conditions on all variables (with the usual normalization condition of the periodic case $\int_\Omega \phi = 0, \ \phi = \mathbf{w}, \mathbf{w}_0, \mathbf{f}$ and q)

The deconvolution problem (2) is typically ill-posed and any method for approximate solution of an ill-posed problem can be tested as a Large Eddy Simulation (LES) model in (3). We study herein the family ($N = 0, 1, 2, \ldots$) of Approximate Deconvolution Models (ADM), introduced in LES by Stolz and Adams [29], [2], based on the van Cittert algorithm, see Bertero and Boccacci [4]. This deconvolution operator satisfies the consistency condition (for $N = 0, 1, 2, \ldots$):

$$\mathbf{u} = D_N(\overline{\mathbf{u}}) + O(\delta^{2N+2}) \qquad \text{for smooth } \mathbf{u},$$

and thus $\overline{\mathbf{u}\,\mathbf{u}} = \overline{D_N(\overline{\mathbf{u}})\,D_N(\overline{\mathbf{u}})} + O(\delta^{2N+2})$. This model has remarkable mathematical properties and its accuracy has been established in the tests of Stolz and Adams [29] ,[2] and the theoretical studies in the work of Dunca and Epshteyn [9] and [18].

In this report, we study the joint energy-helicity cascade for homogeneous, isotropic turbulence generated by the Stolz-Adams approximate deconvolution models (ADM). Our goal is to give a comparison of the energy and helicity statistics of ADM's to the true flow statistics and a comparison of their respective energy and helicity cascades.

Both energy,

$$E(t) := \frac{1}{2L^3} \int_\Omega |\mathbf{u}(\mathbf{x}, t)|^2 \, d\mathbf{x}, \tag{4}$$

and helicity,

$$H(t) := \frac{1}{L^3} \int_\Omega \mathbf{u}(\mathbf{x}, t) \cdot (\nabla \times \mathbf{u}(\mathbf{x}, t)) d\mathbf{x}, \tag{5}$$

3

are conserved by the Euler equations and dissipated (primarily at the small scales) by viscosity. It is widely believed that both cascades, André and Lesieur [1], and the details of their respective cascades are intertwined. Recent studies, confirmed by Bourne and Orszag in [5] have suggested that for homogeneous, isotropic turbulence averaged fluid velocities exhibit a joint energy and helicity cascade through the inertial range of wave numbers given by

$$E(k) = C_E \epsilon^{2/3} k^{-5/3}, \quad H(k) = C_H \gamma \epsilon^{-1/3} k^{-5/3}, \tag{6}$$

where k is wave number, ϵ the mean energy dissipation, and γ the mean helicity dissipation, see also Q. Chen, S. Chen and Eyink [6], Q. Chen, S. Chen, Eyink and Holm [7], Ditlevsen and Giuliani [10]. The cascades are referred to as "joint" because they travel with the same speed through wave space (i.e. the exponents of k are equal). The energy cascade given in (6) is the famous Kolmogorov cascade, and the work of Q. Chen, S. Chen and Eyink [6] showed that the helicity cascade in (6) is consistent for wave numbers up to the standard Kolmogorov wave number, $k_E = \nu^{-3/4} \epsilon^{1/4}$, where ν is the fluid viscosity. Herein, we explore the existence and details of a comparable joint cascade in the ADM (3), to examine if this qualitative feature of the NSE is matched in the ADM.

Exact conservation of helicity for a turbulence model, a first and necessary step for correct helicity cascade statistics, was studied in [27] for the ADM, Leray, Leray-deconvolution, and the Bardina LES models. This work shows that all these models exactly conserve a model mass and model momentum. However, of these only the ADM exactly conserves helicity in the absence of viscosity and external forces, implying that the existence of a helicity cascade is possible.

Other authors have compared LES model energy cascades to energy cascades of the NSE. This was pioneered by Muschinsky [26] for the Smagorinsky model. In [8] by Cheskidov, Holm, Olson and Titi the energy cascade of the Leray-α model was explored, as was the energy cascade of the ADM (3) in [20] and associated regularization in [19]. The work in [20] found that, with some key assumptions, the energy cascade in the ADM is identical to that of the NSE up to the cutoff length scale of δ, and begins to truncate scales like $k^{-11/3}$ for length scales $< \delta$, until viscosity takes over at a length scale larger than $\eta_{Kolmogorov}$. The effects of time relaxation on scale truncation was

explored using similar tools in [19]. There are many other applications of $K41$ phenomenology to understanding LES models, Sagaut [28].

The study of helicity in fluid flow and turbulence has only recently began. It was not until 1961 that helicity's inviscid invariance was discovered by Moreau [25], and two decades later Moffatt gave the topological interpretation of helicity [23] that helicity is nonzero if and only if the flow is not rotationally symmetric. This topological interpretation leads to the commonly accepted interpretation of helicity: it is the degree to which the vortex lines are knotted and intertwined. Another interesting and important feature of helicity is that it is a *rotationally* meaningful quantity that can be checked for accuracy in a simulation. Moffat and Tsoniber gave a good summary of the early results on helicity in [24].

In this study, we show that solutions of the ADM possess a joint energy/helicity cascade that is asymptotically (in the filter width δ) equivalent to that of the NSE. In [20], it is shown that there exists a piecewise cascade for energy in the ADM; that is, up to wave number $\frac{1}{\delta}$, i.e., over the resolved scales, the ADM cascades energy in the same manner as in the NSE ($k^{-5/3}$). However, after this wave number and up to the model's microscale, the ADM cascades energy at a faster rate ($k^{-11/3}$). Interestingly, the results for helicity in the ADM are analogous; helicity is cascaded at the correct rate of $k^{-5/3}$ for wave numbers less than $\frac{1}{\delta}$, and for higher wave numbers up to the model's microscale, helicity is cascaded at a rate of $k^{-11/3}$. This $k^{-11/3}$ rate of enhanced decay is filter dependent, Section 6.1. We deduce the microscale helicity in the ADM and we also show that the helicity cascade is consistent (in the sense introduced by Q. Chen, S. Chen and Eyink [6]) up to the model's energy microscale.

Section 2 gives notation and preliminaries and shows how the deconvolution operator renormalizes the energy. Section 3 gives properties of the ADM, Section 4 derives the joint cascade of energy and helicity in the ADM, Section 5 shows how the ADM truncates scales for helicity, and Section 6 presents conclusions.

2   Notation and Preliminaries

The $L^2(\Omega)$ norm is denoted (as usual) by $\|\phi\| = (\int_\Omega |\phi(x)|^2 \ dx)^{1/2}$ and the deconvolution weighted L^2-norm is denoted by $\|\phi\|_N := (\phi, D_N \phi)^{1/2}$, where D_N is defined precisely in Section 2.2. Every other norm will be explicitly indicated. The space $L_0^2(\Omega)$ contains functions in $L^2(\Omega)$ with zero mean.

Given two real quantities A, B (such as energy and helicity) we shall write

$$A \simeq B$$

if there are positive constants C_1, C_2 depending only on N (which is fixed) with

$$C_1(N)A \le B \le C_2(N)A.$$

For example, in Section 2.2 we show that

$$||\phi|| \le \|\phi\|_N \le \sqrt{N+1}||\phi||, \ \forall \phi \in L^2(\Omega),$$

which is written as $||\phi|| \simeq ||\phi||_N$.

2.1   Nomenclature

The nomenclature used is standard and defined where first used herein. We briefly give a summary of it next.

$\mathbf{u}, p$: The true velocity and pressure, solutions of the underlying Navier-Stokes equations.

$\mathbf{w}, q$: The continuum velocity and pressure predicted by the LES model.

δ : The averaging radius of the filter used in the LES model.

$\widehat{\mathbf{v}}$: The Fourier transform of the function $\mathbf{v}$ for the Cauchy problem and the Fourier coefficient of $\mathbf{v}$ for the periodic problem.

$\mathbf{k}, k$: The dual variable or wave number vector and wave number, respectively;
$$k = |\mathbf{k}| = (\mathbf{k}_1^2 + \mathbf{k}_2^2 + \mathbf{k}_3^2)^{\frac{1}{2}}.$$

$||\mathbf{v}||$: The L^2 norm of the indicated function, $||\mathbf{v}|| = (\int_\Omega |\mathbf{v}(\cdot, t)|^2 \ d\mathbf{x})^{1/2}$.

$||\mathbf{v}||_N$: The deconvolution norm of the indicated function, $||\mathbf{v}||_N = (\mathbf{v}(\cdot, t), D_N \mathbf{v}(\cdot, t))^{1/2}$.

$E(\mathbf{v})(t)$: The true, total kinetic energy of the indicated velocity field at time t:

$$E(\mathbf{v})(t) := \tfrac{1}{2L^3} ||\mathbf{v}(\cdot, t)||^2.$$

$H(\mathbf{v})(t)$: The true, total helicity of the indicated velocity field at time t:

$$H(\mathbf{v})(t) := \tfrac{1}{L^3} \int_\Omega \mathbf{v}(\cdot, t) \cdot (\nabla \times \mathbf{v}(\cdot, t)) d\,\mathbf{x}.$$

$E_{model}(\mathbf{v})(t)$: The kinetic energy of the LES model at time t, given by:

$$E_{model}(\mathbf{v})(t) := \tfrac{1}{2L^3} \{ ||\mathbf{v}(\cdot, t)||_N^2 + \delta^2 ||\mathbf{v}(\cdot, t)||_N^2 \}.$$

$H_{model}(\mathbf{v})(t)$: The helicity of the LES model at time t, given by:

$$H_{model}(\mathbf{v})(t) := \tfrac{1}{L^3} \{ \mathbf{v}(\cdot, t), \nabla \times \mathbf{v}(\cdot, t))_N + \delta^2 (\nabla \times \mathbf{v}(\cdot, t), (\nabla \times)^2 \mathbf{v}(\cdot, t))_N \}.$$

$E(\mathbf{v})(k)$: The distribution of the kinetic energy of the time average of the indicated flow field by wave number.

$H(\mathbf{v})(k)$: The distribution of the helicity of the time average of the indicated flow field by wave number.

$E_{model}(\mathbf{v})(k)$: The distribution by wave number of the LES model's kinetic energy of time or ensemble averages of the indicated flow field.

$H_{model}(\mathbf{v})(k)$: The distribution by wave number of the LES model's helicity of time or ensemble averages of the indicated flow field.

$< \cdot >$: Time averaging of the indicated function,

$$< v >= \limsup_{T \to \infty} \tfrac{1}{T} \int_0^T v(t)\, dt.$$

$\varepsilon(\mathbf{v})(t)$: The (non-averaged) energy dissipation rate,

$$\varepsilon(\mathbf{v})(t) := \tfrac{\nu}{L^3} ||\nabla \mathbf{v}(\cdot, t)||^2.$$

$\gamma(\mathbf{v})(t)$: The (non-averaged) helicity dissipation rate,

$$\gamma(\mathbf{v})(t) := \tfrac{2\nu}{L^3} (\nabla \times \mathbf{v}(\cdot, t), (\nabla \times)^2 \mathbf{v}(\cdot, t)).$$

ε : The mean (time-averaged) energy dissipation rate of the true, Navier-Stokes velocity.

$$\varepsilon :=< \varepsilon(\mathbf{v})(t) > .$$

γ : The mean (time-averaged) energy dissipation rate of the true, Navier-Stokes velocity.

$$\gamma :=< \gamma(\mathbf{v})(t) > .$$

$\varepsilon_{model}(\mathbf{v})(t)$: The (non-averaged) LES model's energy dissipation rate, given by:

$$\varepsilon_{model}(\mathbf{v})(t) := \tfrac{\nu}{L^3}\{||\nabla\mathbf{v}(\cdot,t)||_N^2 + \delta^2||\Delta\mathbf{v}(\cdot,t)||_N^2\}.$$

$\gamma_{model}(\mathbf{v})(t)$: The (non-averaged) LES model's helicity dissipation rate, given by:

$$\gamma_{model}(\mathbf{v})(t) := \tfrac{2\nu}{L^3}\{(\nabla\times\mathbf{v}(\cdot,t),(\nabla\times)^2\mathbf{v}(\cdot,t))_N + \delta^2((\nabla\times)^2\mathbf{v}(\cdot,t),(\nabla\times)^3\mathbf{v}(\cdot,t))_N\}.$$

ε_{model} : The mean (time-averaged) energy dissipation rate of the LES model.

$$\varepsilon_{model} :=< \varepsilon_{model}(\mathbf{v})(t) > .$$

γ_{model} : The mean (time-averaged) helicity dissipation rate of the LES model.

$$\gamma_{model} :=< \gamma_{model}(\mathbf{v})(t) > .$$

$P(\mathbf{v})(t)$: Power input

$$P(\mathbf{v})(t) := \tfrac{1}{L^3}(\mathbf{f}(\cdot,t),\mathbf{v}(\cdot,t)).$$

$P_{model}(\mathbf{v})(t)$: Power input of the LES model

$$P_{model}(\mathbf{v})(t) := \tfrac{1}{L^3}(\mathbf{f}(\cdot,t),\mathbf{v}(\cdot,t))_N.$$

Re : The Reynolds number.

ρ, μ, ν : Respectively, the fluids density, viscosity and kinematic viscosity.

U, L : The large scales characteristic velocity and length scale used to define the Reynolds number.

A : The differential operator that defines the differential filter, $A\mathbf{v} := (-\delta^2\Delta + I)\mathbf{v}$.

G : The filter $G = A^{-1}$.

D_N : The approximate deconvolution operator.

$\overline{\mathbf{v}}$: Overbar denotes the average of the indicated function, $\overline{\mathbf{v}} = G\mathbf{v}$.

$\eta_{Kolmogorov}$: The length scale of the smallest persistent eddies; the Kolmogorov microscale.

k_E : The wave number of the smallest persistent eddies.

η_H : The length scale of the smallest persistent helical structures; analogous to the Kolmogorov microscale for helicity.

k_H : The wave number of the smallest persistent helical structures.

η_{model}^E : The model's energy microscale being the length scale of the model's smallest persistent eddies.

$k_{E_{model}}$: The model's energy wave number being the wave number of the model's smallest persistent eddies.

η^H_{model} : The model's helicity microscale being the length scale of the model's smallest persistent helical structures.

$k_{H_{model}}$: The model's helicity wave number being the wave number of the model's smallest persistent helical structures.

w_{small} : The velocity scale of the smallest persistent eddies in the model's solution.

$[\cdot]$: The units or dimensions.

Re_{small}, Re_{large} : A Reynolds number based on the scales of the smallest/largest persistent eddies.

Remark 1. *For notational compactness, we frequently omit explicit reference to the indicated velocity field. We may write, for instance, $E(t)$ instead of $E(\mathbf{v})(t)$, $H(t)$ instead of $H(\mathbf{v})(t)$, and so on.*

2.2   Norm Equivalence

We focus on the case where averaging is performed by differential filters, Germano [14]. Specifically, given ϕ, $\overline{\phi}$ is the unique L-periodic solution of

$$-\delta^2 \Delta \overline{\phi} + \overline{\phi} = \phi, \qquad \text{in } \Omega, \tag{7}$$

where δ is the selected filter length scale. Differential filters are used, for example, in Q. Chen, S. Chen, Eyink [6], Q. Chen, S. Chen, Eyink and Holm [7], Cheskidov, Holm, Olson, and Titi [8], Dunca and Epshteyn [9], [20], [22], and [27].

Let the averaging operator be denoted by G (so $\overline{\phi} = G\phi := (-\delta^2 \Delta + I)^{-1}\phi$). The basic problem in approximate deconvolution is thus: given $\overline{\phi} = G\phi$ find useful approximations of ϕ. In other words,

$$G\phi = \overline{\phi}, \text{ solve for } \phi.$$

9

For most averaging operators, G is symmetric, positive semi-definite and not stably invertible. Thus, the deconvolution problem is generically ill-posed.

The approximate deconvolution algorithm we consider was studied by van Cittert in 1931. For each $N = 0, 1, ...$, it computes an approximate solution ϕ_N to the above deconvolution equation by N steps of a fixed point iteration, Bertero and Boccacci [4]. Rewrite the above deconvolution equation as the fixed point problem:

$$\text{given } \overline{\phi} \text{ solve } \phi = \phi + \{\overline{\phi} - G\phi\} \text{ for } \phi.$$

The deconvolution approximation is then computed as follows.

Algorithm 2.1 (van Cittert approximate deconvolution algorithm). $\phi_0 = \overline{\phi}$, *where*

for n=1,2,...,N-1, perform

$\phi_{n+1} = \phi_n + \{\overline{\phi} - G\phi_n\}$

$\phi_N = D_N\overline{\phi}$

By eliminating the intermediate steps, the Nth deconvolution operator D_N is

$$D_N\phi := \sum_{n=0}^{N}(I - G)^n\phi. \tag{8}$$

For example, the approximate deconvolution operators corresponding to $N = 0, 1, 2$ are $D_0\overline{\phi} = \overline{\phi}$, and $D_1\overline{\phi} = 2\overline{\phi} - \overline{\overline{\phi}}$, and $D_2\overline{\phi} = 3\overline{\phi} - 3\overline{\overline{\phi}} + \overline{\overline{\overline{\phi}}}$.

Lemma 2.2 (Stability of approximate deconvolution). *Let averaging be defined by the differential filter (7). Then D_N is a self-adjoint, positive semi-definite operator on $L^2(\Omega)$ with norm*

$$||D_N|| := \sup_{\phi \in L^2(\Omega)} \frac{||D_N\phi||}{||\phi||} = N + 1.$$

Proof. We summarize the proof from [3] for completeness. Note that $G := (-\delta^2\Delta + I)^{-1}$ is a self-adjoint positive definite operator with eigenvalues between zero and one, accumulating at zero. Since $D_N := \sum_{n=0}^{N}(I - G)^n$, is a function of G, it is also self-adjoint. By the spectral mapping theorem

$$\lambda(D_N) = \sum_{n=0}^{N} \lambda(I - G)^n = \sum_{n=0}^{N}(1 - \lambda(G))^n.$$

10

Thus, $\lambda(D_N) \geq 0$ and D_N is also positive semi-definite. Since D_N is self-adjoint, the operator norm $||D_N||$ is also easily bounded by the spectral mapping theorem by

$$||D_N|| = \sum_{n=0}^{N} \lambda_{\max}(I - G)^n = \sum_{n=0}^{N}(1 - \lambda_{\min}(G))^n = N + 1. \tag{9}$$

$\square$

Definition 2.3. *The deconvolution weighted norm and inner product are*

$$||\phi||_N = \sqrt{(\phi, D_N\phi)} \quad and \quad (\phi, \psi)_N := (\phi, D_N\psi).$$

for $\phi, \psi \in L^2(\Omega)$.

Lemma 2.4. *We have*

$$||\phi||^2 \leq ||\phi||_N^2 \leq (N+1)||\phi||^2, \quad \forall \phi \in L^2(\Omega) . \tag{10}$$

Proof. As in (9), $1 \leq \lambda(D_N) \leq N + 1$ since

$$\lambda(D_N) = \sum_{n=0}^{N} \lambda(I - G)^n = \sum_{n=0}^{N}(1 - \lambda(G))^n, \text{ and}$$

$$0 < \lambda(G) \leq 1.$$

Since D_N is a self-adjoint operator, this proves the above equivalence of norms. $\square$

It is insightful to consider the Cauchy problem or the periodic problem and visualize the approximate deconvolution operators D_N in wave number space (re-scaled by $k \leftarrow \delta k$). This shows how the N norm reweights the usual $L^2(\Omega)$ norm. The transfer function or symbol of the first three are

$$\widehat{D_0} = 1,$$
$$\widehat{D_1} = 2 - \frac{1}{k^2 + 1} = \frac{2k^2 + 1}{k^2 + 1}, \text{ and}$$
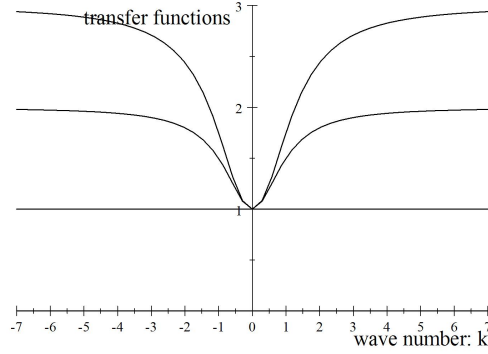$$\widehat{D_2} = 1 + \frac{k^2}{k^2 + 1} + (\frac{k^2}{k^2 + 1})^2.$$

11

Figure 1: Approximate de-convolution operators, N=0,1,2.

Their transfer functions are plotted in figure 1 below.

Note that the plot of $\hat{D}_N(k)$ is consistent with (10): the transfer functions are bounded below by 1, positive and uniformly bounded by $N + 1$. Figure 1 also reveals that the weighted norm is very close to the usual norm on the largest spacial scales but then overweights (by at most $N + 1$) smaller scales.

The large scales are associated with the smooth components and with the wave numbers near zero (i.e., $|\mathbf{k}|$ small). Thus, the fact that D_N is a very accurate solution of the deconvolution problem for the large scales is reflected in the above graph in that the transfer functions $\hat{D}_N(k)$ have high order contact with $\frac{1}{1+k^2}$ near $k = 0$.

Lemma 2.5 (Error in approximate de-convolution). *For any $\phi \in L^2(\Omega)$,*

$$\phi - D_N \overline{\phi} \; = \; (I - A^{-1})^{N+1}\phi$$
$$= \; (-1)^{N+1}\delta^{2N+2}\triangle^{N+1}A^{-(N+1)}\phi,$$

i.e., for smooth ϕ, $\phi = D_N\overline{\phi} + O(\delta^{2N+2})$.

Proof. See Dunca and Epshteyn [9]. □

Proposition 2.6. *For ϕ smooth and N fixed,*

$$\|\phi\|_N^2 = \|\phi\|^2 + O(\delta^2).$$

Proof. This is obvious from figure 1 because $\hat{D}_N(k)$ and 1 have second order contact at $k = 0$. There is a short (but not very insightful) proof using $\phi - \overline{\phi} = O(\delta^2)$ and $\phi - D_N\overline{\phi} = O(\delta^{2N+2})$ as follows:

$$(\phi, D_N\phi) = (\phi, \phi) + (\phi, D_N\overline{\phi} - \phi) + (\phi, D_N(\phi - \overline{\phi})) = \|\phi\|^2 + O(\delta^{2N+2}) + O(\delta^2).$$

$\square$

3 Properties of the Approximate Deconvolution LES Models

The following proposition recalls from Dunca and Epstheyn [9] and [27], respectively, the energy and helicity balances of the ADM (3).

Proposition 3.1 (Model energy and helicity balance). *Consider the ADM (3). The unique strong solution $\mathbf{w}$ of (3) satisfies*

$$\frac{1}{2}[\|\mathbf{w}(t)\|_N^2 + \delta^2\|\nabla\mathbf{w}(t)\|_N^2] + \int_0^t \nu\|\nabla\mathbf{w}(t')\|_N^2 + \nu\delta^2\|\triangle\mathbf{w}(t')\|_N^2 \, dt' =$$

$$= \frac{1}{2}[\|\mathbf{w}_0\|_N^2 + \delta^2\|\nabla\mathbf{w}_0\|_N^2] + \int_0^t (\mathbf{f}(t'), \mathbf{w}(t'))_N \, dt'. \quad (11)$$

$$(\mathbf{w}(t), \nabla \times \mathbf{w}(t))_N + \delta^2(\nabla \times \mathbf{w}(t), (\nabla\times)^2\mathbf{w}(t))_N$$

$$+ 2\nu \int_0^t (\nabla \times \mathbf{w}(t'), (\nabla\times)^2\mathbf{w}(t'))_N + \delta^2((\nabla\times)^2\mathbf{w}(t'), (\nabla\times)^3\mathbf{w}(t'))_N \, dt'$$

$$= (\mathbf{w}_0, \nabla \times \mathbf{w}_0)_N + \delta^2(\nabla\mathbf{w}_0, (\nabla\times)^2\mathbf{w}_0)_N + \int_0^t (\mathbf{f}(t'), \mathbf{w}(t'))_N \, dt' \quad (12)$$

Proof. See Dunca and Epshteyn [9] for the energy equality and [27] for the helicity balance.

$\square$

Remark 2. *From this proposition, we can clearly identify the analogs in the ADM (3) of the physical quantities of kinetic energy, energy dissipation rate, helicity, helicity dissipation rate, and power input, given next.*

Definition 3.2.

$$E_{model}(t) \quad := \quad \frac{1}{2L^3}\{||\mathbf{w}(t)||_N^2 + \delta^2||\nabla\mathbf{w}(t)||_N^2\} \tag{13}$$

$$\varepsilon_{model}(t) \quad := \quad \frac{\nu}{L^3}\{||\nabla\mathbf{w}(t)||_N^2 + \delta^2||\triangle\mathbf{w}(t)||_N^2\} \tag{14}$$

$$H_{model}(t) \quad := \quad \frac{1}{L^3}\{\mathbf{w}(t), \nabla\times\mathbf{w}(t))_N + \delta^2(\nabla\times\mathbf{w}(t), (\nabla\times)^2\mathbf{w}(t))_N\} \tag{15}$$

$$\gamma_{model}(t) \quad := \quad \frac{2\nu}{L^3}\{(\nabla\times\mathbf{w}(t), (\nabla\times)^2\mathbf{w}(t))_N + \delta^2((\nabla\times)^2\mathbf{w}(t), (\nabla\times)^3\mathbf{w}(t))_N\} \tag{16}$$

$$P_{model}(t) \quad := \quad \frac{1}{L^3}(\mathbf{f}(t), \mathbf{w}(t))_N \tag{17}$$

Proposition 3.3. *For smooth* $\mathbf{w}$,

$$E_{model}(t) = E(t) + O(\delta^2), \qquad \varepsilon_{model}(t) = \varepsilon(t) + O(\delta^2),$$

$$H_{model}(t) = H(t) + O(\delta^2), \qquad \gamma_{model}(t) = \gamma(t) + O(\delta^2)$$

$$P_{model}(t) = P(t) + O(\delta^2).$$

Proof. This follows directly from the Definition 3.2, Proposition 2.6 and Lemma 2.5. □

Remark 3. *The energy dissipation in the model*

$$\varepsilon_{\ model}(t) := \frac{\nu}{L^3}||\nabla\mathbf{w}(t)||_N^2 + \frac{\nu}{L^3}\delta^2||\triangle\mathbf{w}(t)||_N^2 \tag{18}$$

is enhanced by the extra term (which is equivalent to $\nu\delta^2||\triangle\mathbf{w}(t)||^2$ *). This term acts as an irreversible energy drain localized at large local fluctuations. The kinetic energy of the model has an extra term*

$$E_{\ model}(t) := \frac{1}{2L^3}[||\mathbf{w}(t)||_N^2 + \delta^2||\nabla\mathbf{w}(t)||_N^2] \tag{19}$$

which is uniformly equivalent to $\delta^2||\nabla\mathbf{w}(t)||^2$.

The true kinetic energy ($E(t) := \frac{1}{2L^3}\|\mathbf{w}(t)\|^2$) in regions of large deformations is thus extracted, conserved and stored in the kinetic energy penalty term $\delta^2\|\nabla\mathbf{w}(t)\|^2$.

3.1 Spectral Representation of the Kinetic Energy

In order to represent the true kinetic energy and the model's kinetic energy spectrally, we expand the velocity field $\mathbf{w}(\mathbf{x}, t)$ in Fourier series as follows:

$$\mathbf{w}(\mathbf{x}, t) = \sum_{k}\sum_{|\mathbf{k}|=k} \hat{\mathbf{w}}(\mathbf{k}, t)e^{i\mathbf{k}\cdot\mathbf{x}}, \tag{20}$$

where $\mathbf{k} \in \mathbb{Z}^3$ is the wave number and

$$\hat{\mathbf{w}}(\mathbf{k}, t) = \frac{1}{L^3}\int_{\Omega} \mathbf{w}(\mathbf{x}, t)e^{-i\mathbf{k}\cdot\mathbf{x}}\,d\mathbf{x}$$

are the Fourier coefficients.

Using Parseval's equality

$$\frac{1}{2\,L^3}\|\mathbf{w}(t)\|^2 = \sum_{k}\sum_{|\mathbf{k}|=k} \frac{1}{2}|\hat{\mathbf{w}}(\mathbf{k}, t)|^2\,.$$

The above formula is equivalent to writing

$$E(t) = \frac{2\pi}{L}\sum_{k} E(k, t),$$

where

$$E(k, t) := \frac{L}{2\pi}\sum_{|\mathbf{k}|=k} \frac{1}{2}|\hat{\mathbf{w}}(\mathbf{k}, t)|^2\,.$$

Then, the time averaged kinetic energy is

$$E = <E(t)>, \quad \text{or} \quad E = \frac{2\pi}{L}\sum_{k} E(k),$$

where $E(k) = <E(k, t)>$.

The model's kinetic energy (13) and energy dissipation rate (14) can also be decomposed in Fourier modes.

Proposition 3.4. *In Fourier space, (13) corresponds to*

$$E_{model}(t) = \sum_k \hat{D}_N(k)\,(1 + \delta^2 k^2)E(k,t), \tag{21}$$

or equivalently,

$$E_{model}(t) = \frac{2\pi}{L} \sum_k E_{model}(k,t), \tag{22}$$

where

$$E_{model}(k,t) := \hat{D}_N(k)\,(1 + \delta^2 k^2)E(k,t). \tag{23}$$

Proof. Using Parseval's equality again, we get

$$\frac{1}{2\,L^3}\|\mathbf{w}(t)\|_N = \sum_k \sum_{|\mathbf{k}|=k} \frac{1}{2}\hat{D}_N(k)\,|\hat{\mathbf{w}}(\mathbf{k},t)|^2 \tag{24}$$

and

$$\frac{1}{2\,L^3}\|\nabla\mathbf{w}(t)\|_N = \sum_k \sum_{|\mathbf{k}|=k} \frac{1}{2}\,k^2\,\hat{D}_N(k)\,|\hat{\mathbf{w}}(\mathbf{k},t)|^2\,. \tag{25}$$

Adding (24) and (25) proves the claim. □

Lemma 3.5. *In wave number space, we can rewrite (14), the model's energy dissipation:*

$$\varepsilon_{model}(t) = \nu\frac{2\pi}{L} \sum_k \hat{D}_N(k)\,k^2(1 + \delta^2 k^2)E(k,t). \tag{26}$$

Using (23), equation (26) can be further simplified to

$$\varepsilon_{model}(t) = \nu\frac{2\pi}{L} \sum_k k^2 E_{model}(k,t). \tag{27}$$

Proof. Start with equation (14) and proceed as in the proof of Proposition 3.4. □

Next, we turn to the spectral representation of helicity.

16

3.2 Helical Mode Decomposition

Definition 3.6. *The helical modes* $\mathbf{h}_\pm$ *are orthonormal eigenvectors of the curl operator, i.e.* $i\mathbf{k} \times \mathbf{h}_\pm = \pm k \mathbf{h}_\pm$.

Since $\mathbf{w}$ is incompressible, $\mathbf{k} \cdot \hat{\mathbf{w}}(\mathbf{k}, t) = 0$ and we can write $\hat{\mathbf{w}}(\mathbf{k}, t) = a_+(\mathbf{k}, t)\mathbf{h}_+ + a_-(\mathbf{k}, t)\mathbf{h}_-$. For the spectral decomposition of helicity, we follow Q. Chen, S. Chen and Eyink [6] and Waleffe [30] and expand $\hat{\mathbf{w}}(\mathbf{k}, t)$ in a basis of helical modes. Therefore, velocity and vorticity can be expanded as

$$\mathbf{w}(\mathbf{x}, t) = \sum_k \sum_{|\mathbf{k}|=k} \sum_{s=\pm} a_s(\mathbf{k}, t)\mathbf{h}_s(\mathbf{k})e^{i\mathbf{k}\cdot\mathbf{x}}, \tag{28}$$

$$\nabla \times \mathbf{w}(\mathbf{x}, t) = \sum_k \sum_{|\mathbf{k}|=k} \sum_{s=\pm} s\, k\, a_s(\mathbf{k}, t)\mathbf{h}_s(\mathbf{k})e^{i\mathbf{k}\cdot\mathbf{x}} \tag{29}$$

Similarly,

$$(\nabla\times)^n \mathbf{w}(\mathbf{x}, t) = \sum_k \sum_{|\mathbf{k}|=k} \sum_{s=\pm} s^n k^n a_s(\mathbf{k}, t)\mathbf{h}_s(\mathbf{k})e^{i\mathbf{k}\cdot\mathbf{x}}. \tag{30}$$

Recall first the definition of helicity, equation (5), for the model's velocity $\mathbf{w}$. Expanding $\mathbf{w}$ in helical modes, we get

$$H(t) = \frac{2\pi}{L}\sum_k H(k, t),$$

where

$$H(k, t) := s\, k\, \frac{L}{2\pi} \sum_{|\mathbf{k}|=k} \sum_{s=\pm} |a_s(\mathbf{k}, t)|^2.$$

Proposition 3.7. *The model's helicity spectrum,* $H_{model}(k, t)$ *is related to the true helicity spectrum,* $H(k, t)$, *as*

$$H_{model}(k, t) = \hat{D}_N(k)(1 + \delta^2 k^2)H(k, t). \tag{31}$$

Proof. Using (28)-(30), we have

$$\frac{1}{L^3}(\mathbf{w}(t), \nabla \times \mathbf{w}(t))_N = \sum_k \sum_{|\mathbf{k}|=k} \sum_{s=\pm} s\hat{D}_N(k)k\,|a(\mathbf{k}, t)|^2$$

and

$$\frac{1}{L^3}(\nabla \times \mathbf{w}(t), (\nabla\times)^2\mathbf{w}(t))_N = \sum_k \sum_{|\mathbf{k}|=k} \sum_{s=\pm} s\hat{D}_N(k)k^3 \left|a(\mathbf{k},t)\right|^2$$

so that

$$H_{model}(t) = \frac{2\pi}{L} \sum_k H_{model}(k,t) = \frac{2\pi}{L} \sum_k \hat{D}_N(k)(1+\delta^2 k^2)H(k). \tag{32}$$

$\square$

Corollary 3.8. $H_{model}(k,t)$ and $H(k,t)$ satisfy $H_{model}(k,t) \simeq (1+\delta^2 k^2)H(k,t)$:

$$(1+\delta^2 k^2)H(k,t) \leq H_{model}(k,t) \leq (N+1)(1+\delta^2 k^2)H(k,t). \tag{33}$$

Proof. By Lemma 2.2, $1 \leq \hat{D}_N(k) \leq N+1$ is bounded. $\square$

Lemma 3.9. *In wave number space, we can rewrite (16), the model's helicity dissipation:*

$$\gamma_{model}(t) = \nu \sum_k \sum_{|\mathbf{k}|=k} \sum_{s=\pm} \hat{D}_N(k)\, sk^3(1+\delta^2 k^2) \left|a_s(\mathbf{k},t)\right|^2. \tag{34}$$

Using (32), equation (34) can be further simplified to

$$\gamma_{model}(t) = \nu\frac{2\pi}{L} \sum_k k^2 H_{model}(k,t). \tag{35}$$

Proof. Use (28)-(30) to write (16) in helical modes. $\square$

4 Phenomenology of the Joint ADM Energy and Helicity Cascade

Since helicity plays a key role in organizing three dimensional flows, it is important to understand the extent to which statistics of helicity predicted by an LES model are correct. We answer that question in this section by extending the similarity theory of approximate deconvolution models (begun in [20]) to elucidate the details of the model's helicity cascade and its connection to the model's energy. Inspired by the earlier work on helicity cascades in the Navier-Stokes equations

done by Brissaud, Frisch, Leorat, Lesieur and Mazure [12], Ditlevsen and Giuliani [10, 11], Q. Chen, S. Chen and Eyink [6], we investigate the existence and details of the joint cascade of energy and helicity for the family of ADM's adapting a dynamic argument of Kraichnan, [16].

Let $\Pi_{model}(k)$ and $\Sigma_{model}(k)$ denote the total energy and helicity transfer from all wave numbers $< k$ to all wave numbers $> k$.

Definition 4.1. *We say that the model exhibits a joint cascade of energy and helicity if in some inertial range, $\Pi_{model}(k)$ and $\Sigma_{model}(k)$ are independent of the wave number, i.e., $\Pi_{model}(k) = \varepsilon_{model}$ and $\Sigma_{model}(k) = \gamma_{model}$.*

Following Kraichnan's formulation of Kolmogorov's ideas of localness of interaction in k space, we assume the following.

Assumption 1. $\Pi_{model}(k)$ $(\Sigma_{model}(k))$ *is proportional to the ratio of the total energy $\sim kE_{model}(k)$ (total helicity $\sim kH_{model}(k)$) available in wave numbers of order k and to some effective rate of shear $\sigma(k)$ which acts to distort flow structures of scale $1/k$.*

The distortion time $\tau(k)$ of flow structures of scale $1/k$ due to the shearing action $\sigma(k)$ of all wave numbers $\leq k$ is given by:

$$\tau(k) \sim \frac{1}{\sigma(k)} \qquad \text{with} \qquad \sigma(k)^2 \sim \int_0^k p^2 E_{model}(p)dp. \tag{36}$$

The conjecture of joint linear cascades of energy and helicity is based on the idea (supported in numerical experiments of Bourne and Orszag [5]) that since energy and helicity are both dissipated by the same mechanism (of viscosity), they relax over comparable time scales.

Assumption 2. $\tau(k)$ *and* $\sigma(k)$ *are the same for energy and helicity of the model.*

We therefore write

$$\Pi_{model}(k) \sim kE_{model}(k)/\tau(k) \qquad \text{and} \qquad \Sigma_{model}(k) \sim kH_{model}(k)/\tau(k). \tag{37}$$

In the definition of mean-square shear (36) the major contribution is from $p \sim k$, in accord with Kolmogorov's localness assumption. This gives

$$\tau(k) \sim k^{-3/2} E_{model}^{-1/2}(k). \tag{38}$$

Putting (37) and (38) together with the fact that $\Sigma_{model}(k) = \gamma_{model}$, it follows that the ADM model helicity spectrum is given by:

$$H_{model}(k) \sim \gamma_{model} k^{-5/2} E_{model}^{-1/2}(k)$$

i.e.,

$$H_{model}(k) \sim \gamma_{model} \varepsilon_{model}^{-1/3} k^{-5/3}. \tag{39}$$

Using relation (33), we write

$$H(k) \sim \frac{\gamma_{model} \varepsilon_{model}^{-1/3} k^{-5/3}}{1 + \delta^2 k^2},$$

which shows that the true helicity spectrum is cut by this family of models as

$$H(k) \quad \sim \quad \gamma_{model} \varepsilon_{model}^{-1/3} k^{-5/3}, \text{ for } k \leq \frac{1}{\delta}, \tag{40}$$

$$H(k) \quad \sim \quad \gamma_{model} \varepsilon_{model}^{-1/3} \delta^{-2} k^{-11/3}, \text{ for } k \geq \frac{1}{\delta}. \tag{41}$$

The above result is depicted in Figure 2.

The energy spectrum $E_{model}(k)$ follows analogously [20]:

$$E_{model}(k) \quad \sim \quad \varepsilon_{model}^{2/3} k^{-5/3}. \tag{42}$$

Further,

$$E(k) \quad \sim \quad \varepsilon_{model}^{2/3} k^{-5/3}, \text{ for } k \leq \frac{1}{\delta}, \tag{43}$$

$$E(k) \quad \sim \quad \varepsilon_{model}^{2/3} \delta^{-2} k^{-11/3}, \text{ for } k \geq \frac{1}{\delta}. \tag{44}$$

Thus, down to the cutoff length scale (or up to the cutoff wave number) the ADM predicts the correct energy and helicity cascades.
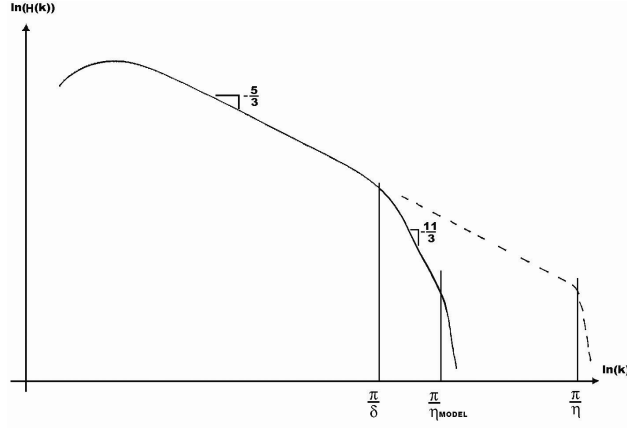
Figure 2: The helicity spectrum of Approximate Deconvolution Models

5   Model's Helicity Microscale and Consistency of the Cascade

On a small enough scale, viscosity grinds down all the flow's organized structures (including helicity) and ends all cascades (including the helicity cascade). The length scale, η_H, at which helical structures do not persist and begin to decay exponentially fast is called the helicity microscale (in analogy with the Kolmogorov microscale for kinetic energy). The correct estimate of the helicity microscale for the NSE is unclear: two estimates with strong arguments in favor of each appear in the literature. The microscale has been estimated for isotropic turbulence by Ditlevsen and Giuliani in [10] to be different (larger) from the Kolmogorov scale $\eta_{Kolmogorov}$: $\eta_H \sim \nu^{-3/7}\gamma^{3/7}\epsilon^{-2/7}$ based on the decomposition of helicity flux in $\pm$ helical modes. On the other hand, Q. Chen, S. Chen and Eyink in [6] show that the net helicity flux is constant up to $\eta_{Kolmogorov}(= k_E^{-1})$, so there is no shorter inertial range for helicity cascade.

In this section, we find that the same occurs when one computes the model's helicity microscale. Based on the equilibrium of the helicity flux, we derive a model's helicity microscale,

η^H_{model}, whereas we show that the model's helicity cascade derived in Section 4 is consistent up to $k_{E_{model}}(= (\eta^E_{model})^{-1})$, in the sense introduced by Q. Chen, S. Chen and Eyink in [6]. These two results do not contradict each other.

5.1 Model's helicity microscale

Using ideas in [20] from the derivation of the energy microscale, η^E_{model}, we estimate the ADM's helicity microscale to be:

$$\eta^H_{model} \sim Re^{-3/11}\delta^{6/11}L^{5/11}, \qquad \text{if } \delta < \eta^H_{model}$$

$$\eta^H_{model} \sim Re^{-3/5}L, \qquad \text{if } \delta > \eta^H_{model}$$

Let the reference velocity and length scale for the large scales be U, L, and $w_{small}, \eta^H_{model}$, for the small scales. From [20] the analog of the small scales and large scales Reynolds number of the model. Recall that these are given by

$$Re_{large} \sim \left.\frac{|\text{nonlinearity}|}{|\text{viscous terms}|}\right|_{\text{large scales}}, \qquad Re_{small} \sim \left.\frac{|\text{nonlinearity}|}{|\text{viscous terms}|}\right|_{\text{small scales}}.$$

Definition 5.1.

$$Re_{model-Large} = \frac{UL}{\nu(1+(\frac{\delta}{L})^2)} \qquad and \qquad Re_{model-Small} = \frac{w_{small}\eta^H_{model}}{\nu(1+(\frac{\delta}{\eta^H_{model}})^2)} \qquad (45)$$

The ADM's energy and helicity cascade are halted by viscosity grinding down eddies exponentially fast. This occurs when $Re_{model-Small} \sim O(1)$, that is, when

$$\frac{w_{small}\eta^H_{model}}{\nu(1+(\frac{\delta}{\eta^H_{model}})^2)} \sim 1. \qquad (46)$$

Equation (46) determines w_{small}

$$w_{small} \sim \frac{\nu(1+(\frac{\delta}{\eta^H_{model}})^2)}{\eta^H_{model}}. \qquad (47)$$

The next important equation to determine the helicity microscale comes from statistical equilibrium of the helicity flux: the helicity input at the large scales must match helicity dissipation at the

22

microscale. The rate of helicity input to the largest scales is the total helicity over the associated time scales

$$\frac{H_{model}}{(\frac{L}{U})} = \frac{\frac{U^2}{L}(1 + (\frac{\delta}{L})^2)}{(\frac{L}{U})} = \frac{U^3}{L^2}\left(1 + \left(\frac{\delta}{L}\right)^2\right). \tag{48}$$

Helicity dissipation at the model's microscale scales as

$$\gamma_{small} \sim \nu \left(\frac{w_{small}^2}{(\eta_{model}^H)^3}\left(1 + \left(\frac{\delta}{\eta_{model}^H}\right)^2\right)\right).$$

This must match the helicity input. There are three cases with the third being the only important one: $\delta = O(\eta_{Kolmogorov})$, $\delta = O(L)$ and the typical case of δ in the inertial range: $\eta_{Kolmogorov} << \delta << L$. If $\delta \sim O(\eta_{Kolmogorov})$, then the simulation reduces to a direct numerical simulation of the NSE. If $\delta \sim O(L)$, then we do not have LES, but VLES (Very Large Eddy Simulation). In the case of VLES, results follow similarly to those below, but are omitted here.

In the case $\delta = O(\eta_{Kolmogorov})$, we have

$$\left(1 + \left(\frac{\delta}{L}\right)^2\right) \sim 1 \text{ and } \left(1 + \left(\frac{\delta}{\eta_{model}^N}\right)^2\right) \sim 1.$$

Thus, at statistical equilibrium,

$$\frac{U^3}{L^2} \sim \nu \frac{w_{small}^2}{(\eta_{model}^H)^3}.$$

Since w_{small} simplifies to ν/η_{model}^H, we get

$$\eta_{model}^H \sim Re^{-3/5}L.$$

In the most important case,

$$\eta_{model}^H << \delta << L$$

we have

$$\left(1 + \left(\frac{\delta}{L}\right)^2\right) \sim 1 \text{ and } \left(1 + \left(\frac{\delta}{\eta_{model}^H}\right)^2\right) \sim \left(\frac{\delta}{\eta_{model}^H}\right)^2.$$

Matching helicity microscale dissipation to large scale input thus simplifies in this case to

$$\frac{U^3}{L^2} \sim \nu \frac{w_{small}^2 \delta^2}{(\eta_{model}^H)^3(\eta_{model}^H)^2}. \tag{49}$$

23

Further, when $\eta_{Kolmogorov} << \delta << L$, the small scale velocity in (47) reduces to

$$w_{small} \sim \frac{\nu\delta^2}{(\eta_{model}^H)^3}.$$ (50)

Substituting (50) into (49) gives

$$\frac{U^3}{L^2} \sim \frac{\nu^3\delta^6}{(\eta_{model}^H)^{11}}.$$ (51)

Solving (51) for η_{model}^H, and using $Re = LU/\nu$ gives the model's helicity microscale,

$$\eta_{model}^H \sim Re^{-3/11}\delta^{6/11}L^{5/11}.$$ (52)

The ADM helicity microscale is slightly larger than the ADM energy microscale (found in [20]): $\eta_{model}^E \sim Re^{-3/10}L^{4/10}\delta^{6/10}$. Hence, capturing wave numbers up to the highest energetic wave number will also capture all wave numbers containing significant helicity.

5.2 Consistency of the ADM joint cascade

The model's energy and helicity dissipation rates are given by equations (27) and (35) above, which are equivalent to

$$\varepsilon_{model}(t) = \nu \int_0^\infty k^2 E_{model}(k,t)dk.$$ (53)

and

$$\gamma_{model}(t) = \nu \int_0^\infty k^2 H_{model}(k,t)dk.$$ (54)

Lemma 5.2. *The wavenumber of the energy microscale of the ADM model (3) is given by*

$$k_{E_{model}} \sim \nu^{-3/4}\epsilon_{model}^{1/4}.$$

Proof. Based on (53), the mean (time-averaged) energy dissipation equals to

$$< \varepsilon_{model}(t) >= \nu \int_0^{k_{E_{model}}} k^2 E_{model}(k)dk,$$

24

where the upper limit of the integral is $k_{E_{model}}$, the wave number of the smallest persistent scales in the model's solution. Using also (42) we derive the estimate for $k_{E_{model}}$ in the usual way as k_E was derived for NSE.

$$< \varepsilon_{model}(t) >\sim \nu k_{E_{model}}^3 E_{model}(k_{E_{model}}) \sim \nu k_{E_{model}}^3 (\epsilon_{model}^{2/3} k_{E_{model}}^{-5/3}) \sim \epsilon_{model}.$$

Solving for $k_{E_{model}}$ gives the result. $\qquad\qquad\square$

Since we have $< \gamma_{model}(t) >= \gamma_{model}$ and the RHS can be calculated by spectral integration through the inertial range, checking this equality is a way to test if the estimate derived for the end of the inertial range is correct (or consistent).

Lemma 5.3. *Provided the largest wave number containing helicity is no larger than k_{Emodel}:*

$$< \gamma_{model}(t) >= \gamma_{model}.$$

Proof. Substituting the helicity cascade result (39) and evaluating the integral (54) up to k_{Emodel} gives

$$\begin{aligned}
< \gamma_{model}(t) > \quad &\sim \quad \nu \gamma_{model} \epsilon_{model}^{-1/3} (k_{Emodel}^{4/3}) \\
&\sim \quad \nu \gamma_{model} \epsilon_{model}^{-1/3} \nu^{-1} \epsilon_{model}^{1/3} \\
&\sim \quad \gamma_{model}
\end{aligned}$$

$\qquad\qquad\square$

Remark 5.4. *We want to stress out that $< \gamma_{model}(t) >= \gamma_{model}$ only if we integrate up to $k_{E_{model}}$, i.e. only if the end of the inertial range for helicity is the same as the end of the inertial range of energy.*

6   Conclusions

A joint energy and helicity cascade has been shown to exist for homogeneous, isotropic turbulence generated by approximate deconvolution models. The energy and helicity both cascade at the

correct $O(k^{-5/3})$ rate for inertial range wave numbers up to the cutoff wave number of $O(\frac{1}{\delta})$, and at $O(k^{-11/3})$ afterward until the model's energy and helicity microscale. This establishes consistency of the model's helicity and energy cascades with the true cascades of the true, underlying turbulent flow.

Furthermore, a microscale for helicity dissipation has been identified for flows predicted by ADMs. As expected, it is larger than the Kolmogorov scale (i.e. the ADM truncates scales) and the microscale for energy dissipation in the ADM (i.e. capturing all scales containing energy will also capture all scales containing helicity).

6.1   Other Filters

With the differential filter (7), scales begin to be truncated by the model at the lengthscale $l = O(\delta)$ by an enhanced decay of the energy and helicity cascade of $k^{-11/3}$. Examining the derivation, the exponent $-11/3$ $(= -5/3 + (-2))$ occurs because the filter decays as k^{-2}. With a fourth order differential filter, these results would be modified to $k^{-14/3}$ $(-14/3 = -5/3 + (-4))$ between the cutoff wavenumber and the microscale. Continuing, it is clear that with the Gaussian filter (which decay exponentially after $k_C = 1/\delta$), exponential decay begins at $k_C = 1/\delta$. In other words, with the Gaussian filter, $k_C = 1/\delta = 1/\eta^H_{model} = 1/\eta^E_{model}$.

7   References

References

[1] J. C. André and M. Lesieur, Influence of helicity on high Reynolds number isotropic turbulence. *Journal of Fluid Mechanics*, 81(1977): 187-207.

[2] N.A. Adams and S. Stolz, Deconvolution methods for subgrid-scale approximation in large eddy simulation, *Modern Simulation Strategies for Turbulent Flow*, R.T. Edwards, 2001.

[3] L. C. Berselli, T. Iliescu, and W. Layton, Mathematics of Large Eddy Simulation of Turbulent Flows. Springer, Berlin, 2006.

[4] M. Bertero and B. Boccacci, *Introduction to Inverse Problems in Imaging*, IOP Publishing Ltd., 1998.

[5] J. Bourne and S. Orszag, Spectra in helical three-dimensional homogeneous isotropic turbulence, *Physics Review Letters E*, 55 (1997): 7005-7009.

[6] Q. Chen, S. Chen, and G. Eyink, The joint cascade of energy and helicity in three dimensional turbulence, *Physics of Fluids*, 2003, Vol. 15, No. 2: 361-374.

[7] Q. Chen, S. Chen, G. Eyink, and D. Holm, Intermittency in the joint cascade of energy and helicity, *Physical Review Letters*, 2003, 90: 214503.

[8] A. Cheskidov, D. D. Holm, E. Olson and E. S. Titi, On a Leray-α model of turbulence, *Royal Society London, Proceedings, Series A, Mathematical, Physical and Engineering Sciences, 461*, 2005, 629-649.

[9] A. Dunca, Y. Epshteyn, On the Stolz-Adams deconvolution LES model, to appear in: SIAM J. Math. Anal., 2006.

[10] P. Ditlevsen and P. Giuliani, Cascades in helical turbulence, *Physical Review E*, Vol. 63, 2001.

[11] P. Ditlevsen and P. Giuliani, Dissipation in helical turbulence, *Physics of Fluids*, 13, 2001.

[12] A. Brissaud, U. Frisch, J. Leorat, M. Lesieur, A. Mazure, Helicity cascades in fully developed isotropic turbulence, *Physics of Fluids*, Vol. 16, Number 8, 1973.

[13] U. Frisch, *Turbulence*. Cambridge University Press, 1995.

[14] M. Germano, Differential filters for the large eddy numerical simulation of turbulent flows. *Physics of Fluids*, 29(1986):1755-1757.

[15] V. John, Large Eddy Simulation of Turbulent Incompressible Flows. *Analytical and Numerical Results for a Class of LES Models*, Lecture Notes in Computational Science and Engineering, vol. 34, Springer-Verlag Berlin, Heidelberg, New York, 2003.

[16] R. Kraichnan, Inertial-range transfer in two- and three- dimensional turbulence, *J. Fluid Mech.*, 47, 525 (1971).

[17] W. Layton and R. Lewandowski, A simple and stable scale similarity model for large eddy simulations: energy balance and existence of weak solutions, Applied Math. Letters 16 (2003), 1205-1209.

[18] W. Layton and R. Lewandowski, Residual stress of approximate deconvolution large eddy simulation models of turbulence. Technical report, 2005, to appear in J. of Turbulence.

[19] W. Layton and M. Neda, Truncation of scales by time relaxation, To appear in *Journal of Mathematical Analysis and Applications*, 2006.

[20] W. Layton and M. Neda, The energy cascade for homogeneous, isotropic turbulence generated by approximate deconvolution models. Technical report, 2006.

[21] M. Lesieur, O. Métais, P. Comte, *Large-Eddy Simulations of Turbulence*, Cambridge, 2005.

[22] C. C. Manica and S. Kaya Merdan, Convergence Analysis of the Finite Element Method for a Fundamental Model in Turbulence, technical report 2006, submitted.

[23] H. Moffatt, Simple topological aspects of turbulent vorticity dynamics, *Proc. IUTAM Symposium on Turbulence and Chaotic Phenomena in Fluids* (ed. T. Tatsumi), pp. 223-230, Elsevier, 1984.

[24] H. Moffatt and A. Tsoniber, Helicity in laminar and turbulent flow. *Annual Review of Fluid Mechanics*, 1992, 24:281-312.

[25] J.J. Moreau, Constantes d'unilot tourbilloinnaire en fluide parfait barotrope, C.R. Acad.Aci. Paris 252, 1961, 2810-2812.

[26] A. Muschinsky, A similarity theory of locally homogeneous and isotropic turbulence generated by a Smagorinsky-type LES, JFM 325 (1996), 239-260.

[27] L. Rebholz, Conservation Laws of turbulence models. To appear in *Journal of Mathematical Analysis and Applications*, 2006.

[28] P. Sagaut, *Large Eddy Simulation for Incompressible Flows*, Springer-Verlag Berlin Heidelberg New York, 2001.

[29] S. Stolz and N.A. Adams, On the approximate deconvolution procedure for LES, *Physics of Fluids*, 11(1999): 1699-1701.

[30] F. Waleffe, The nature of triad interactions in homogeneous turbulence, *Phys. Fluids A*, 4, 350, 1992.